Int. J. Solids Structures Vol. 23, No. 9, pp. 1235-1246, 1987
Printed in Great Britain.

0020-7683/87 $3.00+ .00

AN EXACT TWO-DIMENSIONAL APPROACH TO FIBER MICRO-BUCKLING

PAUL S. STEIF
Department of Mechanical Engineering, Carnegie-Mellon University, Pittsburgh, PA 15213, U.S.A.

(*Received* 2 *July* 1986)

Abstract—Fiber micro-buckling is studied within the context of a two-dimensional (lamellar) model. A bifurcation approach, which rigorously accounts for finite strains and material nonlinearity in both constituents, is employed to examine the possibility of shear and extensional micro-buckling modes. Numerical results for a range of material and geometric parameters are presented, and an asymptotic bifurcation condition is developed for long wavelength shear modes. It is found that shear modes are preferred at higher fiber volume fractions and extensional modes at lower fiber fractions. However, the transition fiber volume fraction, which depends strongly on material nonlinearity, may be higher than previously expected. The distinction between mechanical loading and thermal loading (where one constituent goes into tension and one into compression) is also touched upon briefly.

1. INTRODUCTION

Failure in fiber-reinforced composites can occur in a variety of ways, depending on the loading being sustained. One failure mode postulated to occur under compression parallel to the fibers is fiber micro-buckling[1]. The earliest analysis of this phenomenon appears to be that by Rosen[2], who treated the composite as consisting of two-dimensional laminae and approximated the deformation as that of a beam on an elastic foundation. The buckling condition was based on an energy criterion. Chung and Testa[3] also considered a lamellar structure and performed a bifurcation style analysis in the spirit of Biot[4]. While they took account of finite deformations in the matrix, they continued to treat the fiber as a beam. Three-dimensional treatments of fiber buckling have also been pursued[5–7]. Inevitably, these approaches involve approximating the fiber as a one-dimensional continuum, and they sometimes neglect fiber interactions or tensile deformation in the matrix.

Clearly, a full understanding of micro-buckling will require an adequate account of the three-dimensionality of the problem. In this paper, however, we take the view that a more precise treatment of the relevant buckling modes in a compressed lamellar solid can give qualitative insight into a number of aspects of micro-buckling. The method employed here is similar to that used by Hill and Hutchinson[8] to investigate bifurcation phenomena in a solid subjected to plane strain tension. Their method was recently extended in Refs [9–11] to solve several bimaterial problems. Studying the micro-buckling problem enables us to consider a number of issues including: in-phase (shear) vs out-of-phase (extensional) buckling; the existence of long wavelength modes; the effect of material nonlinearity; and, the distinction between mechanical and thermal loading.

2. FIELD EQUATIONS

The composite, idealized as an infinite layered solid, is shown schematically in Fig. 1. The materials constituting the perfectly bonded alternating layers, labelled A and B, are taken to be time independent and incompressible. Up to the current instant, the solid has been subjected to a uniform in-plane compression parallel to the layers. With regard to incremental deformations from the current state, the materials are assumed to be orthotropic, with stress and strain rates related according to

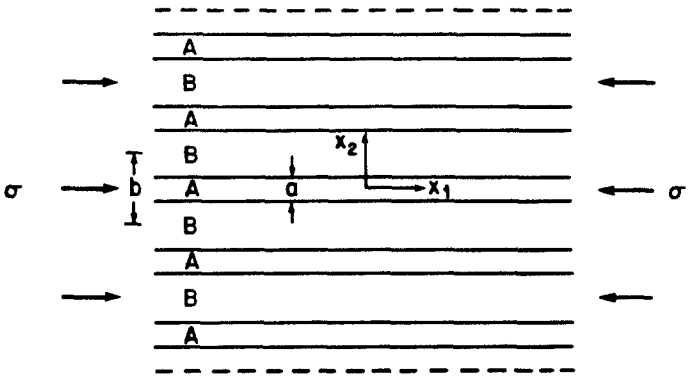

Fig. 1. Schematic of layered solid under compression.

$$D\sigma_{11}/Dt - D\sigma_{22}/Dt = 2\mu^*(\varepsilon_{11}-\varepsilon_{22}), \qquad D\sigma_{12}/Dt = 2\mu\varepsilon_{12} \tag{1}$$

where ε_{ij} are Cartesian components of the Eulerian strain rate, $D\sigma_{ij}/Dt$ are the components of the Jaumann derivative of the true (Cauchy) stress, and subscripts i and j take on the values 1 and 2. The materials are incrementally isotropic when the moduli μ^* and μ are equal. The true stresses in the x_1–x_2 plane at the current instant are taken to be $\sigma_{11} \equiv \sigma$ (<0) and $\sigma_{22} = 0$ (plane strain, uniaxial compression). Note that σ, μ and μ^* are, in general, different in A and B.

By virtue of incompressibility, the velocities v_i (displacement increments) are derivable from a stream function $\psi(x_1, x_2)$ according to

$$v_1 = \frac{\partial\psi}{\partial x_2}, \qquad v_2 = -\frac{\partial\psi}{\partial x_1}.$$

Incremental equilibrium is expressed most conveniently in terms of the nominal stress rates (see Ref. [8] for more details). With the nominal stress rates written in terms of the velocities and, thus, in terms of ψ, one finds that the incremental deformations satisfy equilibrium if

$$\left(\mu+\frac{1}{2}\sigma\right)\frac{\partial^4\psi}{\partial x_1^4} + 2(2\mu^*-\mu)\frac{\partial^4\psi}{\partial x_1^2\partial x_2^2} + \left(\mu-\frac{1}{2}\sigma\right)\frac{\partial^4\psi}{\partial x_2^4} = 0. \tag{2}$$

Conditions which enforce continuity of nominal traction rates and velocities at the interfaces are

$$\left[\left[\left(\mu-\frac{1}{2}\sigma\right)\left\{\frac{\partial^2\psi}{\partial x_2^2}-\frac{\partial^2\psi}{\partial x_1^2}\right\}\right]\right] = 0 \tag{3a}$$

$$\left[\left[\left(4\mu^*-\mu-\frac{1}{2}\sigma\right)\frac{\partial^3\psi}{\partial x_1^2\partial x_2} + \left(\mu-\frac{1}{2}\sigma\right)\frac{\partial^3\psi}{\partial x_2^3}\right]\right] = 0 \tag{3b}$$

$$\left[\left[\frac{\partial\psi}{\partial x_1}\right]\right] = 0 \tag{3c}$$

$$\left[\left[\frac{\partial\psi}{\partial x_2}\right]\right] = 0 \tag{3d}$$

where [[ ]] denotes the difference in the values of the enclosed quantity at the interface as one approaches from A and from B. It will be useful below to introduce the quantities

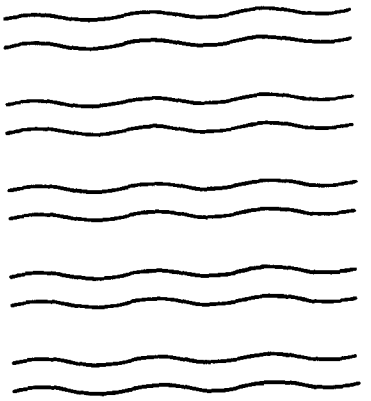

Fig. 2(a). In-phase buckling mode.

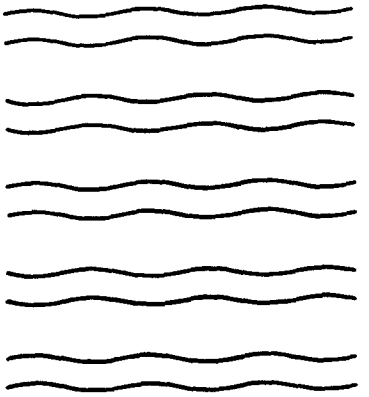

Fig. 2(b). Out-of-phase buckling mode.

$$R \equiv \frac{\mu}{2\mu^*}, \qquad S \equiv \frac{\sigma}{4\mu^*}, \qquad \xi \equiv \frac{\mu_B^*}{\mu_A^*}.$$

3. EIGENMODES

Two types of micro-buckling modes are frequently cited as arising from the compression of a fiber composite. The first mode, called the in-phase (shear) mode, is shown schematically in Fig. 2(a). This mode involves deformations in both A and B which are anti-symmetric about their center lines. The second mode, called the out-of-phase (extensional) mode, is shown in Fig. 2(b). Here, the deformation of one constituent is anti-symmetric about its center line, and the other constituent deforms in a symmetric fashion. Both modes are periodic in the x_1-direction and can be written in the form

$$\psi = f(x_2) \sin \frac{2\pi x_1}{\lambda} \tag{4}$$

where $f(x_2)$ is defined piecewise in A and B.

In-phase and out-of-phase modes are distinguished by the functions $f(x_2)$. Without loss of generality, we take the layer A to deform anti-symmetrically in both modes, thus

$$f_A(x_2) = \mathrm{Re}\left[c \cos \frac{2\pi}{\lambda} \alpha x_2\right] \tag{5}$$

where

$$\alpha^2 = \frac{R_A - 1 + \sqrt{(S_A^2 - 2R_A + 1)}}{R_A - S_A}.$$

Then, for the in-phase mode we have

$$f_B(x_2) = \text{Re}\left[d \cos \frac{2\pi}{\lambda}\beta\left(\frac{b}{2} - x_2\right)\right] \tag{6a}$$

while for the out-of-phase mode we have

$$f_B(x_2) = \text{Re}\left[d \sin \frac{2\pi}{\lambda}\beta\left(\frac{b}{2} - x_2\right)\right] \tag{6b}$$

where

$$\beta^2 = \frac{R_B - 1 + \sqrt{(S_B^2 - 2R_B + 1)}}{R_B - S_B}.$$

As discussed in some detail by Hill and Hutchinson[8], eqn (2) is elliptic, hyperbolic or parabolic depending on the values of R and S. We concentrate on a subset of the various possibilities by confining attention to the elliptic regime in which $R > 1$ and $S^2 < 2R - 1$ in both A and B. The hyperelastic solids studied most extensively here fall into this category. In such cases, α and β are complex, and, without loss of generality, the first quadrant roots may be used.

From continuity conditions (3), one finds the bifurcation equations to be satisfied are

$$\text{Re}\{c\alpha[-(R_A - S_A)\alpha^2 + (R_A + S_A - 2)] \sin \alpha q_A\} = \xi\ \text{Re}\{d\beta[(R_B - S_B)\beta^2 - (R_B + S_B - 2)] \sin \beta q_B\} \tag{7a}$$

$$(R_A - S_A)\ \text{Re}[c(1 - \alpha^2) \cos \alpha q_A] = \xi(R_B - S_B)\ \text{Re}[d(1 - \beta^2) \cos \beta q_B] \tag{7b}$$

$$\text{Re}[c \cos \alpha q_A] = \text{Re}[d \cos \beta q_B] \tag{7c}$$

$$-\text{Re}[c\alpha \sin \alpha q_A] = \text{Re}[d\beta \sin \beta q_B] \tag{7d}$$

for the in-phase mode, and

$$\text{Re}\{c\alpha[(R_A - S_A)\alpha^2 - (R_A + S_A - 2)] \sin \alpha q_A\} = \xi\ \text{Re}\{d\beta[(R_B - S_B)\beta^2 - (R_B + S_B - 2) \cos \beta q_B]\} \tag{8a}$$

$$(R_A - S_A)\ \text{Re}[c(1 - \alpha^2) \cos \alpha q_A] = \xi(R_B - S_B)\ \text{Re}[d(1 - \beta^2) \sin \beta q_B] \tag{8b}$$

$$\text{Re}[c\alpha \sin \alpha q_A] = \text{Re}[d\beta \cos \beta q_B] \tag{8c}$$

$$\text{Re}[c \cos \alpha q_A] = \text{Re}[d \sin \beta q_B] \tag{8d}$$

for the out-of-phase mode. We have defined the normalized wave numbers q_A and q_B to be

$$q_A \equiv \frac{\pi a}{\lambda}, \qquad q_B \equiv \frac{\pi(b - a)}{\lambda}.$$

First, we consider the existence of long wavelength modes, i.e. solutions for λ arbitrarily large. For the case of in-phase modes, one finds the bifurcation condition in the long wavelength limit ($q_A \to 0$ and $q_B \to 0$) to be

$$(\mu_A - \tfrac{1}{2}\sigma_A)\sigma_A + (\mu_B - \tfrac{1}{2}\sigma_B)\sigma_B + 2(\mu_A - \tfrac{1}{2}\sigma_A)(\mu_B - \tfrac{1}{2}\sigma_B)$$
$$+ h_r(\mu_A - \tfrac{1}{2}\sigma_A)(\mu_B + \tfrac{1}{2}\sigma_B) + \frac{1}{h_r}(\mu_A + \tfrac{1}{2}\sigma_A)(\mu_B - \tfrac{1}{2}\sigma_B) = 0 \quad (9)$$

where

$$h_r \equiv \frac{b-a}{a}.$$

On the other hand, an examination of eqns (8) reveals that a long wavelength mode is not possible for out-of-phase modes. From a more physical viewpoint, a long wavelength (diffuse) mode involves a homogeneous deformation which is different than the remotely applied strain. For out-of-phase buckling, this is precluded by the condition of $v_2 = 0$ at $x_2 = \pm b/2$, since continuity of v_2 at $x_2 = \pm a/2$ would force material B to undergo a volume change which violates incompressibility. Indeed, the combined conditions of incompressibility and interfacial continuity insure that there are no long wavelength versions of a number of different modes in layered solids[10, 11]. No such restriction exists for the in-phase mode. Whether long wavelength modes are possible gives some information regarding the validity of assuming that the fiber can be approximated as a beam. For long wavelength modes, the deformation varies over a length scale which is long compared with the fiber diameter—a condition crucial to the beam assumption. Thus, for example, one ought to suspect results for the out-of-phase modes which are based on treating the fiber as a beam.

Another interesting feature of the diffuse buckling mode, eqn (9), is that it depends on σ and μ. On the other hand, diffuse necking in a monolithic (or clad) sheet subjected to tension depends on σ and μ*. Thus, while necking in tension is independent of the shearing resistance μ, provided it is finite, in-phase micro-buckling is independent of the tangent modulus associated with continuing compressive deformation. This observation of the influence of anisotropy is not evident from previous work on isotropic materials.

When the constituent materials are hyperelastic and isotropic, the shear modulus μ in uniaxial plane strain tension or compression is given by

$$\mu = \frac{1}{2}\sigma\frac{\lambda^4+1}{\lambda^4-1}$$

where σ is the stress in uniaxial, plane strain tension or compression, and λ is now the stretch. Since, by continuity at the interface, λ is the same in A and B, eqn (9) reduces to

$$\sigma_B^2(\lambda^4-1) + \sigma_A^2(\lambda^4-1) + \sigma_A\sigma_B\left[2 + \lambda^4\left(h_r + \frac{1}{h_r}\right)\right] = 0. \quad (10)$$

Clearly, there is no long wavelength tensile mode ($\sigma_A > 0$, $\sigma_B > 0$, $\lambda > 1$), but there is a compressive mode ($\sigma_A < 0$, $\sigma_B < 0$, $0 < \lambda < 1$).

An additional simplification is possible when the stress–strain behavior is of the form

$$\sigma = kg(\lambda)$$

where the function $g(\lambda)$ is the same in materials A and B, and k takes on the values k_A and k_B in A and B, respectively. For convenience, let $k_r \equiv k_A/k_B$. Then the critical stretch λ_{cr} is given by

$$\lambda_{cr}^4 = \frac{1-2\eta}{1+(h_r+1/h_r)\eta} \quad (11)$$

where

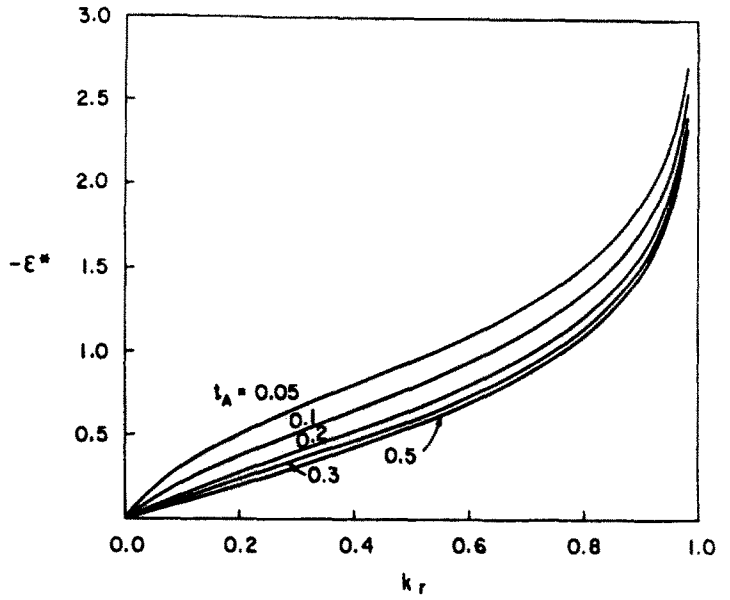

Fig. 3. Long wavelength (in-phase mode) buckling strain as a function of stiffness ratio.

$$\eta = \frac{k_r}{k_r^2 + 1}.$$

We now make contact with the small-strain work of Greszczuk[7] who considers a material composed of linear elastic constituents. If we take

$$\sigma = k\varepsilon \tag{12}$$

where ε is the infinitesimal strain, then the average longitudinal stress, Σ, is given by

$$\Sigma = (k_A t_A + k_B t_B)\varepsilon \tag{13}$$

where t_A and t_B are the respective volume fractions. Also, the average in-plane shear modulus, G, is given by

$$G = \frac{1}{4}\left[\frac{k_A k_B}{k_A t_B + k_B t_A}\right]. \tag{14}$$

The normalized buckling stress Σ/G is then given by

$$\frac{\Sigma}{G} = [t_A^2 + t_B^2 + t_A t_B(k_r + 1/k_r)] \ln\left[\frac{1-2\eta}{1+(h_r+1/h_r)\eta}\right]. \tag{15}$$

In the limit of a very large modulus difference, say $k_r \ll 1$, Greszczuk's result, $\Sigma = G$, is found to hold for all volume fractions.

4. RESULTS

First, we consider results for long wavelength modes under the assumption that $\sigma = kg(\lambda)$. Plotted in Fig. 3 are curves of compressive buckling strain $-\varepsilon^*$ as a function of stiffness ratio k_r for various volume fractions t_A. The strain is taken to be the logarithmic strain $\varepsilon \equiv \ln \lambda$. Only the ranges $0 < k_r < 1$ and $0 < t_A < 0.5$ are shown, since the long wavelength limit (depending on η and $h_r + 1/h_r$) is unaffected by *independent* exchanges of moduli and volume fractions. A *simultaneous* exchange of moduli and volume fractions

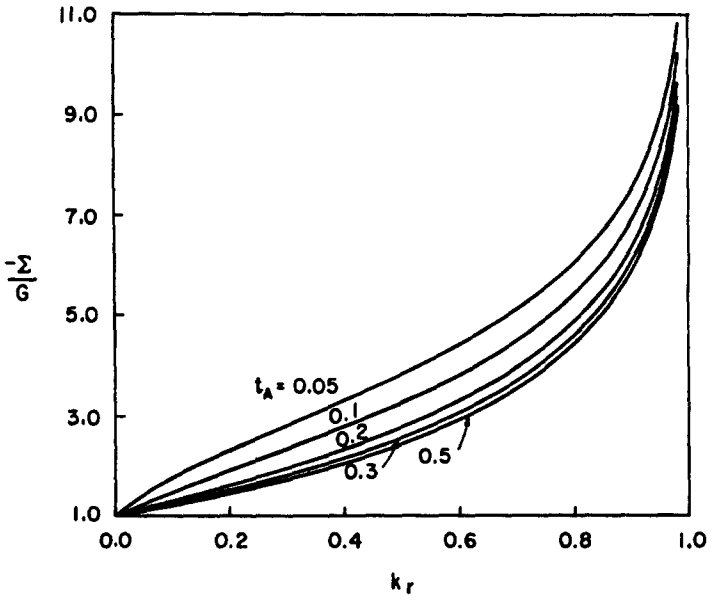

Fig. 4. Long wavelength buckling stress for linear material.

would only involve reversing our choice of which material we refer to as "fiber" and which material we refer to as "matrix"—clearly irrelevant to the in-phase mode involving anti-symmetric deformation in *both* constituents. Being unaffected by *independent* exchanges of moduli and volume fractions means that the buckling strain is the same whether a given constituent occupies a volume fraction t or $1-t$. As seen below, this is not true when modes of finite wavelength are considered. We note further that the buckling strain increases without bound as the moduli become equal and as either volume fraction approaches zero. Even though buckling strains of arbitrary magnitude appear possible from Fig. 3, beyond a certain strain the equations lose ellipticity. In the hyperbolic regime, discontinuous deformation gradients (shear bands) are theoretically possible. Assuming the linear material response, eqn (12), and G given by eqn (14), the normalized buckling stress σ/G can be calculated (Fig. 4). The limiting result $\Sigma = G$ is always exceeded, and by a substantial amount, if k_r is not too different from 1.

We now turn to the results for in-phase finite wavelength modes. Numerical calculations were based on a power-law stress–strain behavior in uniaxial plane strain compression of the form $\sigma = k\varepsilon^N$, where k and N differ in A and B. (The results depend only on k_r, N_A and N_B.) The buckling strain as a function of normalized wave number q_A is shown in Fig. 5 for the case of in-phase buckling modes. To simulate a fiber composite, we take $k_r = 0.05$. Since A is the "stiffer" constituent, we will refer to t_A as the fiber volume fraction. The hardening rates have been chosen to be $N_A = N_B = 0.2$; some of the influence of this nonlinearity is discussed further below. As seen from eqn (11), the buckling strain in the long wavelength limit ($q_A \to 0$) is a minimum at $t_A = 0.5$. Furthermore, the long wavelength buckling strain is unaltered with respect to an exchange of volume fractions ($t_A \leftrightarrow 1 - t_A$). The difference between, say, $t_A = 0.2$ and 0.8 appears at finite wavelengths. For the higher volume fraction, the long wavelength mode has the lowest buckling strain. For low volume fraction composites, a finite wavelength mode has the lowest buckling strain. As the volume fraction is made increasingly small, there is no long wavelength mode in the elliptic regime, but there is a finite wavelength mode. On the other hand, there are no modes whatsoever in the elliptic regime when the fiber fraction is very high.

A somewhat different situation exists with respect to out-of-phase buckling (see Fig. 6). As discussed earlier, there is no long wavelength out-of-phase mode. The first out-of-phase mode to appear is of finite wavelength: for fiber volume fractions in excess of roughly 0.2, the minimum buckling strain increases with increasing fiber volume fraction. Similar to in-phase buckling, there are no modes in the elliptic regime when the fiber volume fraction is very high. This result is reminiscent of the internal necking modes of a layered solid

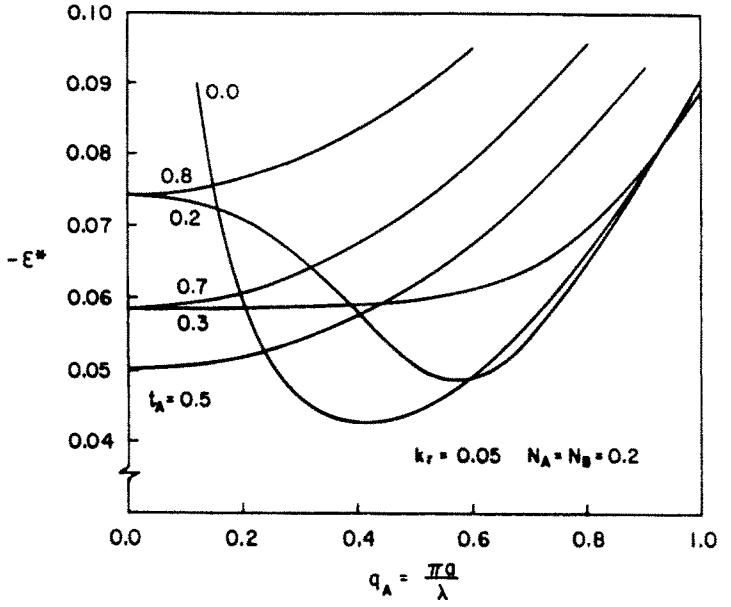

Fig. 5. Buckling strain for finite wavelength in-phase modes.

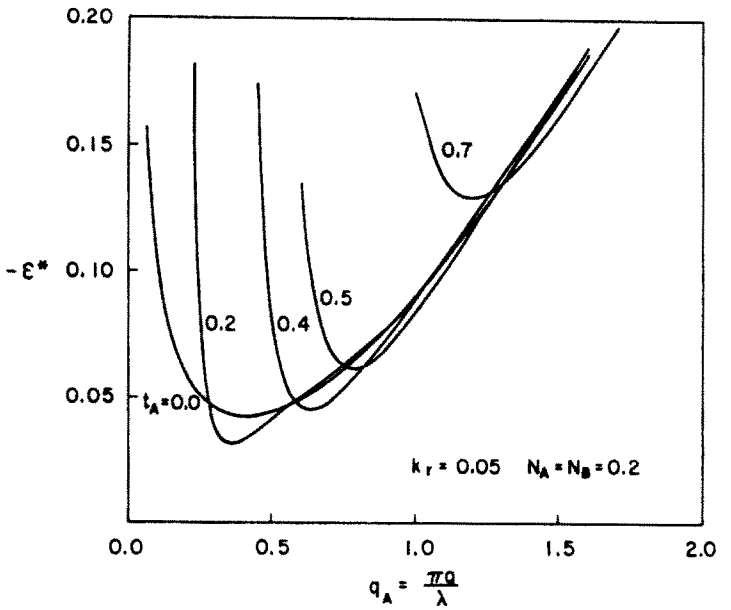

Fig. 6. Buckling strain for finite wavelength out-of-phase modes.

subjected to overall tension parallel to the layering[10]. Necking-type modes were excluded prior to loss of ellipticity when the stiffer constituent constituted a high volume fraction.

It is often stated[12] that in-phase buckling is favored at higher t_A (>0.2), while out-of-phase buckling is favored for low volume fraction composites. We give an example of this trend in Fig. 7, in which we plot in-phase and out-of-phase buckling strains for two different volume fractions, $t_A = 0.3$ and 0.6. (Note that $k_r = 0.05$ and $N_A = N_B = 0.2$.) While the in-phase buckling curves are similar, the out-of-phase buckling curves are quite different. Clearly, the in-phase mode is favored when $t_A = 0.6$, and the out-of-phase mode is favored when $t_A = 0.3$. For the same set of material parameters we have plotted the minimum out-of-phase and minimum in-phase buckling strains as a function of volume fraction (Fig. 8). For volume fractions in excess of, roughly, 0.42, the in-phase mode is favored. We note also that the in-phase mode to appear at the lowest strain is the long wavelength mode when $t_A > 0.29$. As the fiber fraction becomes very small, the in-phase mode again appears before the out-of-phase mode, though only slightly. Of course, as

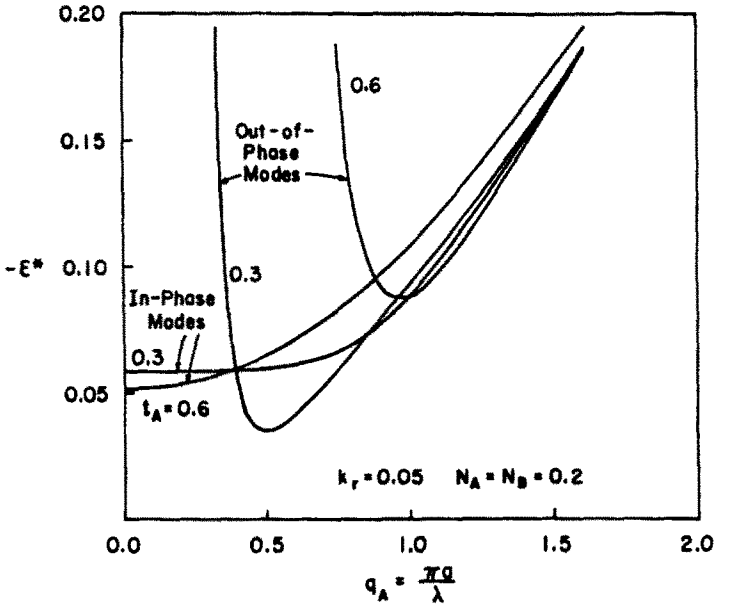

Fig. 7. Comparison of in-phase and out-of-phase buckling strains for different fiber volume fractions.

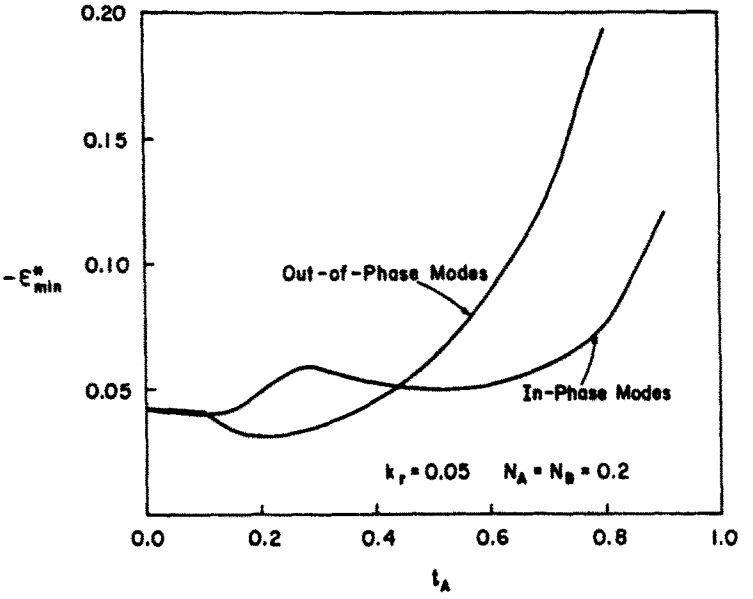

Fig. 8. Minimum in-phase and out-of-phase buckling strains as a function of fiber volume fraction.

$t_A \to 0$, the two modes are identical. As is suggested below, however, the competition between in-phase and out-of-phase modes can be strongly influenced by material nonlinearity.

Some of the influence of material nonlinearity is exhibited in Fig. 9. We have fixed $k_r = 0.05$ and $t_A = 0.5$, and we have plotted bifurcation strains (both in-phase and out-of-phase modes) vs wave number for a range of hardening rates ($N_A = N_B$). To emphasize a point raised earlier, we note that the long wavelength in-phase mode depends on the relative stiffness (k_r) and not on the hardening rate (when $N_A = N_B$). Modes of finite wavelength, whether in-phase or out-of-phase, depend on the hardening rates. Though curves for a variety of fiber volume fractions are not shown, it can be readily deduced by comparing Figs 7 and 9 that the volume fraction which must be exceeded to have the in-phase mode appear first increases as the hardening decreases.

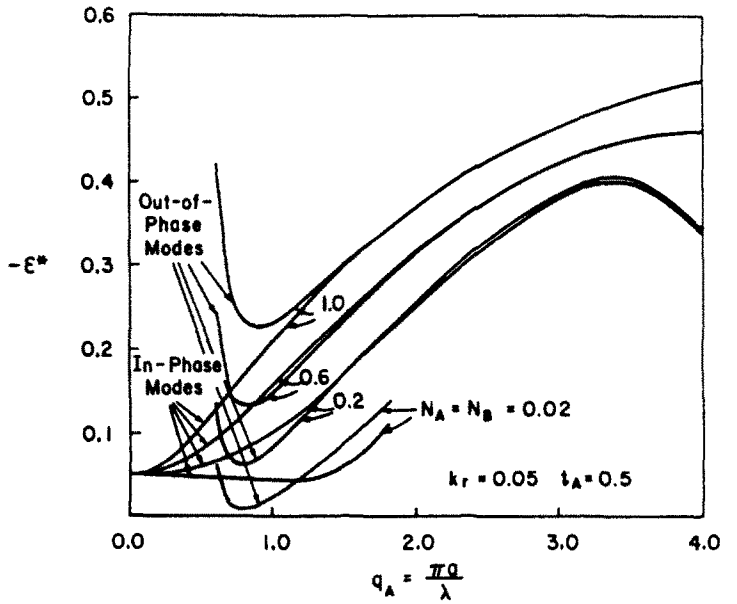

Fig. 9. Effect of material nonlinearity on in-phase and out-of-phase buckling modes.

Finally, we consider the possibility that the loading is not mechanical, but thermal. This is of some importance, since tests suggested by Rosen[2] involve inducing fiber micro-buckling via thermal loading. Say the stress is zero everywhere in the composite at some given temperature. Let the temperature be altered. If the constituents have different thermal expansions, then one constituent will go into tension and one into compression, in such a way that the composite will still have zero net load on it. First, it is possible to draw some immediate conclusions regarding the possibility of long wavelength in-phase modes. Whatever the particular values of σ_A and σ_B, they must satisfy the zero load condition

$$\sigma_A t_A + \sigma_B t_B = 0.$$

With this relation, one finds that the left-hand side of the long-wavelength bifurcation condition (10) is always of one sign; thus, one deduces that no long wavelength mode is possible.

For $k_r = 0.05$, $N_A = N_B = 0.2$ and $t_A = 0.5$, calculations have been carried out for a number of situations shown in Table 1. The results are shown in Fig. 10. There are a variety of combinations because either the fiber or the matrix can be in compression (the other being in tension), and, independently, either can be the anti-symmetrically deforming constituent. We found that there are no elliptic regime bifurcations when the fiber deforms symmetrically and is in compression.

For the purposes of comparison, Fig. 10 also includes bifurcation results for mechanical loading of the same composite, in which case the stress in both constituents is compressive. In order of increasing minimum bifurcation strain, the modes (induced by mechanical loading) are: in-phase; out-of-phase with the fiber deforming anti-symmetrically; and, out-of-phase with the fiber deforming symmetrically. That the last mode emerges at a significantly higher strain means that it is the fiber that "buckles", not the matrix. Any intuition gained from considering the results of mechanical loading appears to be relatively useless when turning to examine thermal loading. One can say that if the fiber goes into

Table 1

T1	In-phase	fiber in compression	
T2	In-phase	fiber in tension	
T3	Out-of-phase	fiber in compression	deforms anti-symmetrically
T4	Out-of-phase	fiber in tension	deforms anti-symmetrically
T5	Out-of-phase	fiber in tension	deforms symmetrically

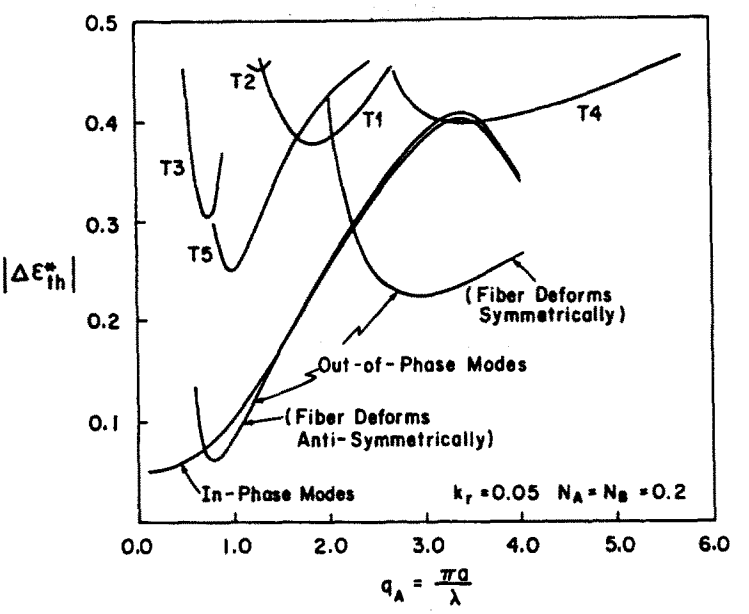

Fig. 10. Comparison of buckling strains under thermal and mechanical loading.

compression, then the out-of-phase mode is predicted to emerge first, though at a strain considerably higher than when the composite sustains mechanical loading. On the other hand, if the fiber goes into tension, the first mode to emerge is an out-of-phase mode involving buckling of the matrix. This suggests that one treat predictions based on mechanical loading with caution when applying them to thermal loading.

5. CONCLUSIONS

This paper has shown that two-dimensional micro-buckling involving linear or nonlinear constituents can be treated exactly within a classic bifurcation framework. Both in-phase (shear) modes and out-of-phase (extensional) modes are possible, though only for the in-phase mode does there exist a mode of arbitrarily long wavelength. In the long-wavelength limit, the buckling stress equals the composite shear modulus for a linear material ($\sigma = k\varepsilon$), provided the stiffness of the two constituents are very different. Roughly speaking, in-phase modes are favored when the fiber volume fraction is high, while out-of-phase modes are favored at low volume fractions. However, the transition fiber volume fraction can vary quite widely, depending on the material nonlinearity. It was found that inducing strain via temperature change, which puts one constituent into tension and one into compression, results in very different buckling strains than does mechanical loading. In any event, we share the conclusion reached by previous investigators that the compressive stress needed to produce micro-buckling is far higher than observed compressive strengths. Though this suggests that micro-buckling may not be the cause of compressive failure, it is also possible that the perfect bonding of the constituents assumed here and elsewhere, which puts severe constraint on buckling modes, is not realistic[12].

Acknowledgements—This work has been supported by the National Science Foundation under grant MSM-8451080, by the General Electric Engine Business group, by the Alcoa Technical Center and by the Department of Mechanical Engineering, Carnegie–Mellon University.

REFERENCES

1. N. F. Dow and I. J. Gruntfest, Determination of most needed potentially possible improvements in materials for ballistic and space vehicles. GE-TIS 60SD389 (June 1960).
2. B. W. Rosen, Mechanics of composite strengthening. In *Fiber Composite Materials*, Chap. 3. ASM, Metals Park, Ohio (1965).
3. W.-Y. Chung and R. B. Testa, The elastic stability of fibers in a composite plate. *J. Comp. Mater.* **3**, 58 (1969).

4. M. A. Biot, *Mechanics of Incremental Deformation*. Wiley, New York (1965).
5. M. A. Sadowsky, S. L. Pu and M. A. Hussain, Buckling of microfibers. *J. Appl. Mech.* **34,** 1011 (1967).
6. L. R. Herrmann, W. E. Mason and S. T. K. Chan, Response of reinforcing wires to compressive states of stress. *J. Comp. Mater.* **1,** 212 (1967).
7. L. B. Greszczuk, Microbuckling failure of circular fiber-reinforced composites. *AIAA J.* **13,** 1311 (1975).
8. R. Hill and J. W. Hutchinson, Bifurcation phenomena in the plane tension test. *J. Mech. Phys. Solids* **23,** 239 (1975).
9. P. S. Steif, Bimaterial interface instabilities in plastic solids. *Int. J. Solids Structures* **22,** 195 (1986).
10. P. S. Steif, Periodic necking instabilities in layered plastic composites. *Int. J. Solids Structures* **22,** 1571 (1986).
11. P. S. Steif, Deformation instabilities in clad metal subjected to rolling. *J. Appl. Metalworking* **4,** 317 (1987).
12. L. B. Greszczuk, On failure modes of unidirectional composites under compressive loading. In *Fracture of Composite Materials* (Edited by G. C. Sih and V. P. Tamuzs), pp. 231–244. Martinus Nijhoff, The Hague (1982).